Shock-wave-induced enhancement of optical emission in nitrogen afterglow plasma

N. Siefert,* B. N. Ganguly, and P. Bletzinger
Air Force Research Laboratory, Building 450, Wright-Patterson Air Force Base, Ohio 45433, USA
(Received 27 April 2005; published 6 December 2005)

This paper reports measurements of optical emission enhancement at the shock front of Mach 1.5 to Mach 3.5 shockwaves propagating in the afterglow of a 0.75 Torr nitrogen glow discharge. Electrically-generated shocks pass through the afterglow and create noticeable enhancements of the $B\,^3\Pi_g$-$A\,^3\Sigma_u^+$ and $C\,^3\Pi_u$-$B\,^3\Pi_g$ transitions of nitrogen. Under our discharge conditions, the electron Debye length was approximately the same magnitude as the shock thickness; this allows the possibility of a space-charge region extending beyond the neutral shockwave discontinuity. Previous researchers have measured enhancement in the $B\,^3\Pi_g$-$A\,^3\Sigma_u^+$ optical emission at the shock front, but only in the active discharge. Fibers connected to photomultipler tubes measure the optical emission from the discharge. Laser deflection measures the shock velocity. The data reveals that the emission enhancement increases with Mach number, and also indicates that the emission enhancement decreases exponentially with time in the afterglow. Since the discharge voltage has already been shut off, the energy needed to create the emission enhancement cannot come from the power supply. We conclude that under our discharge conditions there is an increase in the already non-equilibrium energy of the electrons at the shock front via a shockwave-induced strong double layer.

DOI: 10.1103/PhysRevE.72.066402 PACS number(s): 52.70.Kz, 52.35.Tc, 52.80.Hc, 82.33.Xj

I. INTRODUCTION

Interactions of weakly ionized gases (ionization fraction, $\alpha=10^{-6}-10^{-8}$) with weak shockwaves ($1<\mathrm{Mach}<4$) have been studied over the last thirty years. Initially, the focus was on plasma modification of shock properties, such as shock velocity and shock stand-off distance [1,2]. For discharges operating at low reduced electric fields ($E/N<10^{-16}$ V cm^2), Ionikh *et al.* [3] demonstrated both experimentally and numerically that the dominant mechanism for shock modification is the increase in the global gas temperature. The goal of the present work was *not* to study how weakly ionized plasma affects global shock properties, but rather the goal was to understand how a weak shockwave affects plasma properties at the shock front. To our knowledge, there has been no reported enhancement of optical light emission in the afterglow and no reported enhancement in $C\,^3\Pi_u$-$B\,^3\Pi_g$ emission in either the active discharge or the afterglow.

Early analytic attempts by Greenberg *et al.* [4] and Jafrin [5] to determine the charge separation and self-consistent electric field at the shock front in weakly ionized plasma ($\alpha=10^{-3}$) assumed that the electron and ion temperatures were equal and assumed that the electron Debye length was much smaller than the region of the neutral shockwave discontinuity. The electric fields were quite large; however, since the Debye lengths were quite small, the potential differences were confined to roughly $2kT_e/e$, where kT_e is the electron temperature and e is the electric charge. In the shock reference frame, the electric field in Refs. [4,5] is an ambipolar electric field that prevents the electrons from diffusing out of the shock front. As in the case of the ambipolar electric field in the radial direction of the positive column in a glow discharge, the electric field at the shock front in Refs. [4,5] retards the thermal diffusion of electrons. The ambipolar radial electric field decelerates energetic electrons, and hence, the electric fields calculated in Refs. [4,5] cannot account for the emission enhancement at the shock front presented in this paper.

Previous analytic and numerical studies are also unable to explain the optical emission enhancement seen by Bletzinger *et al.* [6] at the shock front in a weakly ionized, nitrogen glow discharges. Under these conditions, the electrons were not in thermal equilibrium with neutrals and ions either before or after the shock front. At a pressure of 5 Torr and with the discharge still on, the production of both excitation and ionization at the shock front was polarization dependent; for example, there was a roughly 25% difference in emission enhancement depending on whether the shockwave traveled from the anode to the cathode or from the cathode to the anode [6,7]. They concluded that an electric field was set up at the shock front that accelerated rather than decelerated the electrons.

The first aim of this research was to report an emission enhancement at the shock front, even though the voltage across the discharge has been shut off. This was to demonstrate that the energy needed for the emission enhancement was not coming from the power supply. The second aim was to investigate how the emission enhancement scales as a function of Mach number and as a function of the decay time in the afterglow. The third aim was to rule out the compression of electrons and/or metastable states as the possible cause of the emission enhancement. Usually, an increase in the electron-neutral collision frequency behind the shock front brings the system into thermal equilibrium at a faster rate and, hence, causes a decrease in light emission behind the shock front. However, our results demonstrate that under certain conditions there is an increase in the already nonequilibrium energy of the electrons at the shock front. Collisions between neutrals and positive ions set up a space-charge re-

*Electronic mail: Nicholas.Siefert@wpafb.af.mil

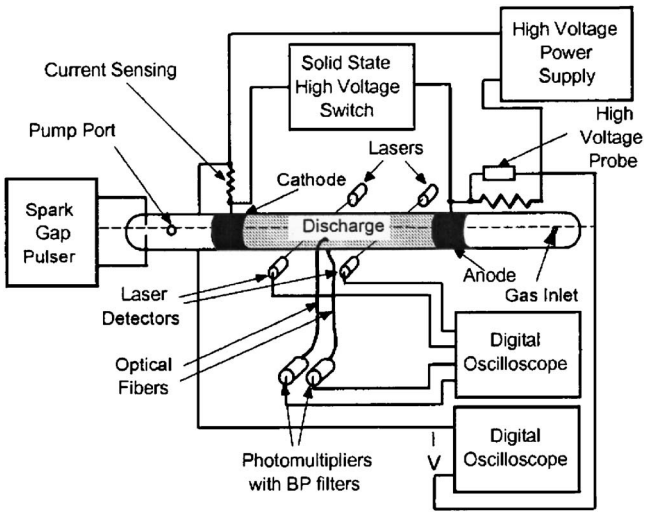

FIG. 1. Schematic of experiment. Note: the optical fibers are colocated with the He–Ne laser closest to the spark-gap pulser.

gion that accelerates electrons. Put another way, there is a collective uphill pumping of energy from the "colder" neutral particles ($\sim$0.1 eV) to the "hotter" electrons ($\sim$1 eV) via the positive ions.

II. EXPERIMENTAL SETUP

Figure 1 shows the schematic of the experimental set up. The set up is broken down into the following: direct current (DC) glow discharge with two cylindrical electrodes, two lasers for measuring the shock velocity, two optical fibers connected to photomultiplier tubes (PMTs) for measuring optical emission, a coaxial spark gap for generating the shockwave, and a high voltage switch for shutting off the discharge.

The DC active discharge was created between two conformal wall electrodes spaced 30 cm apart. The radius of the glass tube was 1.5 cm. To prevent the accumulation of impurities in the discharge, the gas was pumped through the tube at a rate of 20 standard cubic centimeters per minute (sccm). The gas flow and pressure were regulated by an electronic flowmeter and a downstream flow controller. The gas pressure of the system was 0.75 Torr, which was monitored with a capacitance manometer. The current in the discharge before shutting off was 20 mA, corresponding to a current density of 3 mA/cm^2. Two wires placed inside the glass tube measured the voltage difference in the positive column before the glow discharge was shut off. The wires were separated by 2 cm and were connected to 1000X, 100 MΩ high voltage probes. The voltage difference divided by the distance between the wires provided the axial electric field in the positive column. In all cases, the electric field before shutting off the discharge was kept constant at 24.5 ± 0.5 V/cm, which corresponds to an E/N value of roughly 100 Td (1 Td$=1\times10^{-17}$ V cm^2). The experimentally derived values for the reduced electric field and the current density were used as input parameters to BOLSIG, a numerical discharge code [8]. The numerically determined, average electron energy was 2.8 eV. The peak electron number density was 1.7×10^9 cm^{-3}. The electron Debye length before switching off the discharge is 0.3 mm and the fraction of ionization is 10^{-7}. The neutral-neutral collision mean free path upstream of the shock front is 0.6 mm, and downstream of the shock front, the mean free path is between 0.1 and 0.3 mm, depending on Mach number. Since the electron temperature stays around 1 eV in the nitrogen afterglow [9], the electron Debye length is comparable to the shock front thickness for these experimental conditions.

As discussed in Ref. [2], a helium-neon laser beam was passed perpendicularly across the discharge to determine the arrival of the shockwave. This beam was directed unto a photodiode such that the photodiode signal jump was approximately proportional to the line-averaged density gradient jump [10]. This pulse determines the location of the shock front. The width of the laser beam was 1 mm, leading to a time resolution of 1 μs for a shock velocity of 1 km/s. Temporal signals from two laser beams, spaced 4 cm apart, measured the average shock velocity between the two lasers. To convert the shock velocity into a Mach number, it was necessary to determine the gas temperature inside the glow discharge. This was estimated from the energy balance between the input power and the conductive heat loss. The mean temperature inside the discharge was calculated by solving for the transport of Joule heat via conduction to the walls, as detailed by Raizer [11]. The estimated mean temperature was $360\ \mathrm{K} \pm 20$ K at a current of 20 mA. The speed of sound in the discharge was therefore, on average, 375 m/s. This value was used to convert the shock velocity measured by the helium-neon lasers into a Mach number. Under our discharge conditions, the ion temperature is roughly equal to the neutral gas temperature. Therefore, the mean electron energy is roughly ninety times larger than the ion mean energy before switching off the discharge.

The indirect evidence for the increase in electron energy at the shock front comes from the enhancement of optical emission. Two fiber optic cables, with collimating lens attached in front, collected photons emitted from the same axial position in the positive column. The spatial resolution of the fibers with the collimating lens was 2 mm. These photons were passed through a filter before being amplified by a PMT. A band pass filter centered on 775.4 nm blocked out all photons except for those corresponding to the $B\ ^3\Pi_g$-$A\ ^3\Sigma_u^+$ transition in nitrogen. A band pass filter centered on 337.1 nm allowed only photons corresponding to the $C\ ^3\Pi_u$-$B\ ^3\Pi_g$ transition to pass through. The 337.1 nm signal was significantly smaller than the 775.4 nm signal. However, the two signals are scaled to the same steady-state amplitude. The $C\ ^3\Pi_u$-$B\ ^3\Pi_g$ emission accurately tracks the emission enhancement at the shock front since the radiative lifetime of the transition [12] is much smaller than the collision quenching time. This is not the case for the $B\ ^3\Pi_g$-$A\ ^3\Sigma_u^+$ transition since its radiative lifetime [12] is comparable to its collision quenching time for gas pressures near and above 1 Torr. The two photo-deflection signals and the two PMT signals are sent to a four channel, 1.5 GHz LeCroy oscilloscope. The current and voltage signals are sent to a two-channel 500 MHz LeCroy oscilloscope.

The shockwaves in this experiment were created with a 2.7 cm diameter coaxial spark gap with an inner tungsten pin

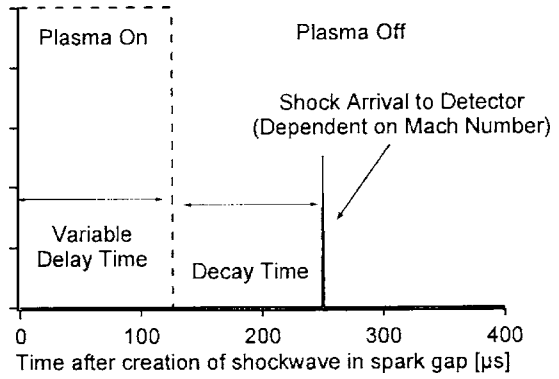

FIG. 2. Time evolution of plasma switching and shock arrival. The time between the creation of the shock in the spark gap, $t=0$ μs, and the switching off of the discharge is labeled the delay time. The time between switching off the discharge and the arrival of the shock front to the viewing volume of the optical fibers and first He–Ne laser is labeled as the decay time. The vertical dash represents the switching-off of the discharge and the pulse represents the arrival of the shock front to the first He-Ne laser.

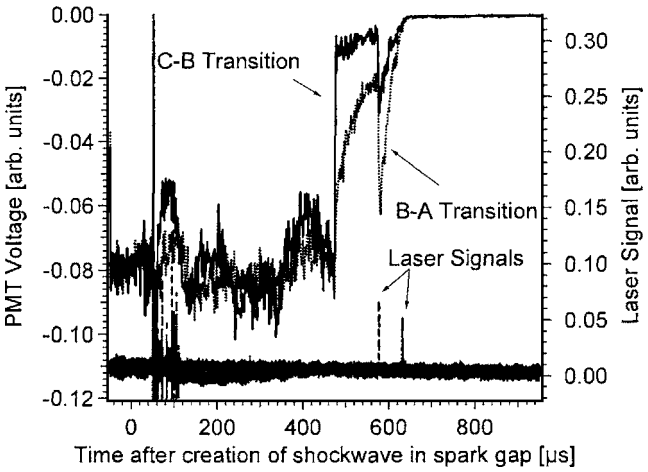

FIG. 3. Example for Mach 1.9 & decay time=100 μs. First laser is aligned with fibers. Second laser is 4 cm downstream. There were significant fluctuations in light emission until the discharge was shut off at $t=472$ μs. Note that the PMT puts out negative voltage when collecting photons.

electrode. A power supply charged up capacitors that deposited up to 350 J of energy in less than 5 μs using an EG&G spark gap switch. The capacitance value was either 2 μF or 7 μF and the voltage was varied from 5 to 10 kV. In this way, the shock velocity could be varied from roughly 500 to 1300 m/s. There was a ninety degree bend in the tube after the spark gap and before the discharge. The bend is not shown in the 2D schematic in Fig. 1. The bend slightly slowed down the shock, but the purpose of the bend was to trap the photons created by the spark gap from reaching the discharge.

The glow discharge was switched off by a high voltage insulated gate bipolar transistor (IGBT). The time between the creation of the shock and the shutting off of the plasma, labeled as the "delay time," was varied in order to vary the time between shut off and shock arrival at the fibers, labeled as the "decay time." Figure 2 shows the time evolution of the plasma switching and the shock front arrival in the viewing volume of the optical fibers. The discharging of the capacitors into the co-axial spark gap was initiated by a pulse/delay generator. This master clock sent out timing signals to the EG&G spark gap, to the oscilloscope, and to the IGBT.

III. RESULTS

Figures 3 and 4 are examples of the raw data coming from the lasers and the PMTs. The PMTs put out a negative voltage when collecting photons. The PMTs recorded a constant, steady state plasma emission value until $t=0$ μs, which corresponded to the creation of the shock in the spark gap. There were some fluctuations in the discharge emission due to radio frequency interference from the creation of the electrically driven shocks. There was a noticeable decrease in the $C\ ^3\Pi_u$-$B\ ^3\Pi_g$ emission within one microsecond after shutting off the discharge, followed by a slower drop with an e-folding decay time of 100 μs. The rapid $C\ ^3\Pi_u$-$B\ ^3\Pi_g$ emission decay within 1 μs is indicative of the decay of electrons with energies above 6 eV [9]. The $B\ ^3\Pi_g$-$A\ ^3\Sigma_u^+$ emission dropped with an e-folding decay time of 100 μs. This measured decay time may have been impacted by a small amount of air impurity in the discharge. In pure nitrogen, Guerra *et al.* [9] reported that the electron temperature in the nitrogen afterglow can remain around 1 eV due to superelastic collisions with $A\ ^3\Sigma_u^+$ metastables and vibrationally excited ground states, which means that the electron Debye length does not significantly decrease after shutting off the discharge. This means that the electron mean energy is roughly thirty times larger than the ion mean energy in the afterglow. The 100 μs decay of the $C\ ^3\Pi_u$-$B\ ^3\Pi_g$ and $B\ ^3\Pi_g$-$A\ ^3\Sigma_u^+$ emission appears to be the convolution of the decay of electron number density via ambipolar diffusion to

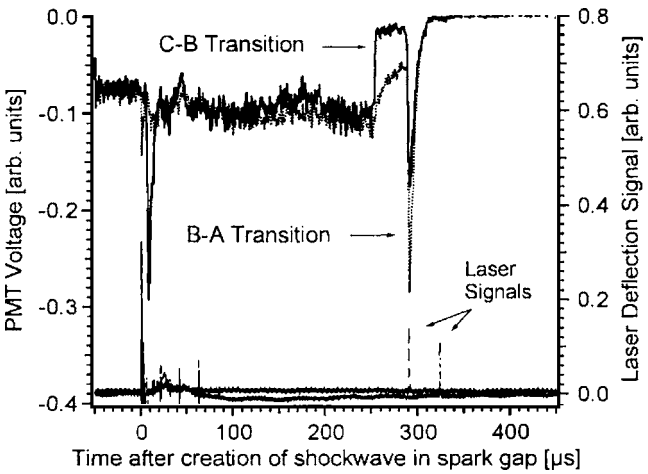

FIG. 4. Example for Mach 3.2 and decay time=40 μs. First laser is aligned with fibers. Second laser is 4 cm downstream. The pulse in the C-B PMT voltage near $t=0$ μs is electrical noise from the spark gap. The discharge was shut off at $t=250$ μs. The light emission peaks well above the steady state. The value of C-B light emission increases sixteen fold across the shock front. Note that the PMT puts out negative voltage when collecting photons.

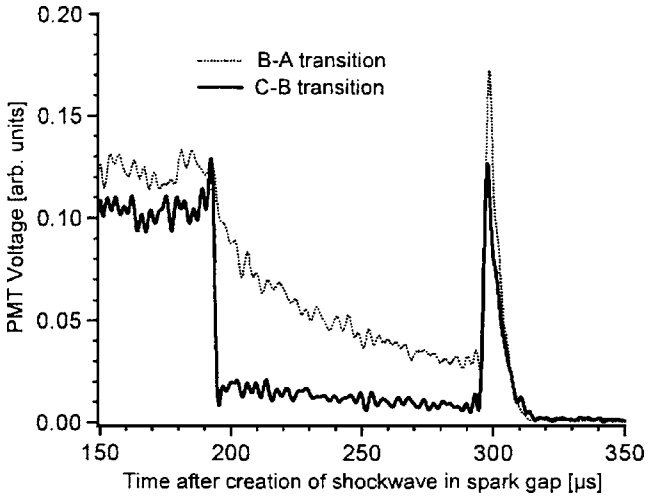

FIG. 5. Zoom-in for Mach 3.4 and decay time=100 μs. Note that the negative PMT signal has been inverted in this graph for clarity. The light emission at the shock front peaks above the steady state. The laser signals are not shown. The discharge was shut off at $t=195$ μs. The value of *C-B* light emission increases thirteen fold across the shock front.

the wall [11] and the decay of the electron temperature in the bulk of the electron energy distribution function [9].

When the shock arrived at the location of the fibers, there were enhancements in both PMT signals and a concurrent jump in the first laser photo-deflection signal. These three detectors are axially colocated within 1 mm. Figure 5 shows a temporally expanded time scale of the emission enhancement at the shock front. For better clarity, we have inverted the PMT signals and have removed the laser signals in Fig. 5. The rise time of emission enhancement for both transitions was 2 μs, regardless of the Mach number or the decay time. Since the spatial resolution of the fiber was 2 mm, the actual rise time may be less than the observed rise time. For higher Mach number and shorter decay time, the emission intensities peaked well above the steady state condition, as shown in Figs. 4 and 5. In fact, in Fig. 4, the $C\ ^3\Pi_u$-$B\ ^3\Pi_g$ emission at the peak of the enhancement is sixteen times larger than the emission intensity immediately before the arrival of the shock front.

Figures 6 and 7 show the trends in the emission enhancement versus Mach number and decay time in the afterglow. For both plots, the left axis is the ratio of the emission jump to the steady state emission. The emission jump was measured as the peak value in emission minus the emission value just before the shock arrived. The steady state value was the value at $t=0$ μs. Dividing by the steady state value, the y axis is a nondimensional variable and factors into account the fact that the $C\ ^3\Pi_u$-$B\ ^3\Pi_g$ emission signal was amplified in order to plot at the same scale as the $B\ ^3\Pi_g$-$A\ ^3\Sigma_u^+$ emission signal. Figure 6 shows the dependence of the emission enhancement on Mach number. For these data points, the time between the plasma switch off and shock arrival at the optical fibers was kept constant at 99±2 μs, implying a constant electron number density and a constant electron temperature when the shockwave arrived into the viewing volume of the fibers. There is an approximately linear

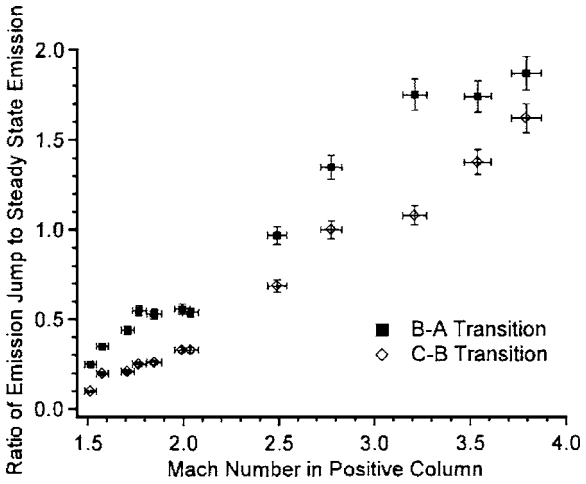

FIG. 6. Dependence of emission enhancement on Mach number. The decay time was held constant at 99 μs±2 μs. There is a linear trend in the emission enhancement versus Mach number.

dependence of the emission enhancement versus Mach number for both transitions. The trend, if continued to lower Mach numbers, suggests that the emission enhancement only occurs for Mach numbers greater than 1. Figure 7 shows the dependence of the emission enhancement on the decay time in the afterglow. For these data points, the shock velocity was kept constant at 1200±20 m/s, which corresponds to Mach 3.2. The decay of the emission enhancement matches the slow 100 μs decay of both the $C\ ^3\Pi_u$-$B\ ^3\Pi_g$ and $B\ ^3\Pi_g$-$A\ ^3\Sigma_u^+$ emission in the afterglow.

IV. DISCUSSION

Before discussing how the formation of a shockwave-induced, strong double layer explains the enhancement of both $B\ ^3\Pi_g$-$A\ ^3\Sigma_u^+$ and $C\ ^3\Pi_u$-$B\ ^3\Pi_g$ emission, we will ana-

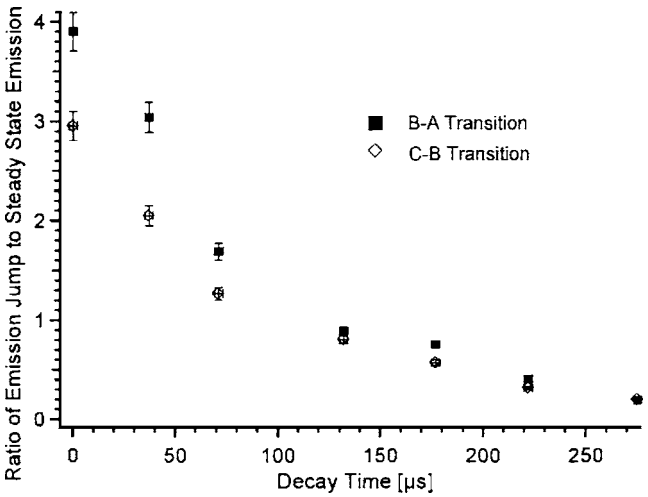

FIG. 7. Dependence of emission enhancement on time in afterglow. Constant shock velocity of 1200 m/s±20 m/s ($M=3.4$). There is an exponential dependence of the emission enhancement on time in the afterglow. The characteristic *e*-folding decay time is roughly 100 μs.

TABLE I. Reactions and rate constants for the creation of the $C\ ^3\Pi_u$ and the $B\ ^3\Pi_g$ states via the $A\ ^3\Sigma_u^+$ mestastable

$N_2(A)+N_2(A)\rightarrow N_2(B)+N_2(X)$	$k_1=7.7\times10^{-11}$ cm^3 s^{-1} (Ref. [14])
$N_2(A)+N_2(A)\rightarrow N_2(C)+N_2(X)$	$k_2=1.5\times10^{-10}$ cm^3 s^{-1} (Ref. [15])
$N_2(X,4<v<15)+N_2(A)\rightarrow N_2(X,v=0)+N_2(B)$	$k_3=2\times10^{-11}$ cm^3 s^{-1} (Ref. [13])

lyze and rule out other possible explanations of the emission enhancement at the shock front. The emission enhancement cannot be due to an increase in electron mean energy due to collisions between electrons and ions or electrons and neutral species. Elastic collisions cause the electrons to lose some of their mean energy ($\sim$1 eV) to heavy particles, whose mean energy behind the shock front is roughly 0.1 eV, depending on Mach number. Also, the emission enhancement cannot be due to an increase in electron mean energy due to converting directed electron energy into thermal electron energy; the shock velocity is roughly 1 km/s and the mean electron thermal speed is 400 km/s. From the electron's perspective, the shockwave is highly subsonic.

Another possible explanation for the emission enhancement would be that the electrons are compressed at the shock front by the $2kT_e/e$ double layer reported in Refs. [4,5]. However, the electric field in Refs. [4,5] is an ambipolar field such that it will decelerate upstream electrons approaching the shock front. The energy to create this ambipolar field would come at the expense of the energetic electrons. Compression of electrons by the $2kT_e/e$ double layer reported in Refs. [4,5] cannot explain the rapid rise in the $C\ ^3\Pi_u$-$B\ ^3\Pi_g$ emission to values greater than the emission signal level before switching off the discharge. For example, in Fig. 4, the $C\ ^3\Pi_u$-$B\ ^3\Pi_g$ emission reached a value sixteen times greater than the emission signal immediately before the arrival of the shock front. According to the Rankine-Hugoniet relationship, the ratio of neutral density after and before a Mach 3.2 shockwave is only 3.3. Compression alone cannot cause an increase in emission by a factor of 16. Yet another evidence against the electron compression effect is the polarization dependence of the excitation and ionization seen by Bletzinger *et al.* [6,7]. Observations presented in this paper and previous papers cannot be explained by compression of electrons by a self-consistent, ambipolar field set up at the shock front.

Since the emission jumps are positively correlated with increasing Mach number, there is another possible mechanism for the enhancement in light emission that does not require a strong double layer. The emission enhancements could be due to the compression of excited neutral species, such as the $A\ ^3\Sigma_u^+$ metastable. The jump condition for the $A\ ^3\Sigma_u^+$ metastable state density is specified by the Rankine-Hugoniet relationship, very similar to the electronic ground-state density. Two $A\ ^3\Sigma_u^+$ metastable states can collide and make either the $B\ ^3\Pi_g$ state or the $C\ ^3\Pi_u$ state, making it possible that the emission enhancement at the shock front is due to the pooling of $A\ ^3\Sigma_u^+$ metastable states. However, this mechanism can be ruled out for two reasons.

First, the rate of pooling of excited neutral species is too slow. Table I shows three main processes for creating $B\ ^3\Pi_g$ and $C\ ^3\Pi_u$ states using a combination of $A\ ^3\Sigma_u^+$ metastable states and vibrationally excited ground state molecules. Using the rate constants for the first two reactions listed in Table I and using numerically determined metastable state densities in Ref. [13], the rate to make $B\ ^3\Pi_g$ states is 1.5×10^3 sec^{-1} and the rate to make $C\ ^3\Pi_u$ states is 3×10^3 sec^{-1}. The associated rise times are 600 and 300 μs, respectively. These values are two orders of magnitude slower than the measured 2 μs rise time needed to explain the data. Using Ref. [13] for the density of vibrational states, the rise time for the third equation in Table I is on the order of magnitude of 2 μs. The third equation is the collision of an $A\ ^3\Sigma_u^+$ mestastable state with a vibrationally excited ground state molecule. However, there is no known mechanism that can obtain the 2 μs rise time needed to produce $C\ ^3\Pi_u$ states via collisions of vibrationally excited ground states with metastable states. Therefore, the metastable/vibrational pooling theory cannot explain the rapid rise in the $C\ ^3\Pi_u$-$B\ ^3\Pi_g$ emission. The second reason against metastable pooling is that Bletzinger *et al.* [6] measured a roughly 25% difference in emission enhancement depending on whether the shockwave propagated from the cathode to anode or from the anode to cathode. If the light emission came solely from compression of excited neutral species, then there would be no difference in the light emission enhancement between two possible directions through the discharge.

Although there is no known theoretical foundation for strong double layer formation at a weak collisional shock front, the rapid enhancement of the $C\ ^3\Pi_u$ state, which lies 11 eV above the ground state, is the strongest experimental evidence for a strong double layer ($>10kT_e/e$) that accelerates rather than decelerates the electrons. Since we have ruled out compression of electrons and/or metastable states and since we have conducted the experiments in the afterglow, we infer that the energy source for the emission enhancement is the neutral particle shockwave. Collisions between electrons and nitrogen molecules cannot directly increase the energy of the electrons; however, collisions between neutral species and positive ions can create a region of charge separation at the shock front. This region of charge separation, i.e., a double layer, is a shocklike structure in the electrostatic potential with steep gradients in electron temperature, charge particles number density and light emission [16–18]. The dependence of these variables on the polarity of the discharge current is a characteristic of current-carrying double layers [19]. Conde *et al.* [20] have numerically studied increases of electron impact ionization in weakly ionized plasmas when electrons pass through a strong double layer.

The "nonlocal" electron energy distribution on the high potential side of the double layer resembles the drifted-Maxwellian seen in the cathode of glow discharges and is capable of both ionization and excitation.

The light emission at the shock front shows similar attributes. Figures 3 and 4 suggest that the electron energy increases in the post-shock region because the light emission only appears after the shock front. Figure 6 indicates that the strength of the double layer depends on Mach number. Assuming a no-slip condition between the positive ion density and the neutral ground state density at the shock front, there will be a gradient of ion density at the shock front that depends on Mach number. This steep gradient in ion density will create a region of charge separation. Figure 7 suggests that the mean electron energy must remain around 1 eV in order to see the emission enhancement at the shock front. Bletzinger *et al.* [21] did *not* measure an enhancement in $C\ ^3\Pi_u$-$B\ ^3\Pi_g$ light emission at the shock front in 5 Torr nitrogen discharges, where the reduced electric field (E/N) was significantly lower. Under those discharge conditions, both the electron Debye length and the electron relaxation lengths were smaller than this current experimental condition. We infer from present and past results that collisions between positive ions and neutrals set up a region of space-charge separation and a self-consistent electric field at the shock front that converts a small portion of the energy of the neutral shockwave into increasing the already nonequilibrium energy of the electrons. This type of "up-pumping" of energy is not possible collisionally, but rather is only possible via a collective, long-range interaction, such as an electrical double layer.

V. CONCLUSION

This paper reports indirect evidence for local heating of already nonequilibrium electrons at the shock front, as seen by enhancements of optical emission at the shock front in the afterglow of a nitrogen positive column. This is experimental evidence of light emission enhancement at a weak shock front in the afterglow and for an enhancement in $C\ ^3\Pi_u$-$B\ ^3\Pi_g$ emission at the shock front. The experimental conditions were such that the electron Debye length, prior to shutting off the discharge, was comparable to the shock thickness and such that the mean electron energy was much greater than the ion temperature. For a given time in the afterglow, the emission enhancement increases approximately linear with Mach number; for a given Mach number, the emission enhancement decreases exponentially with time in the afterglow. Since the voltage across the discharge is switched off before the arrival of the shock front, the energy needed to create the emission enhancement cannot come from the power supply. We conclude that under our discharge conditions there is an increase in the already nonequilibrium energy of the electrons at the shock front via a shockwave-induced strong double layer.

ACKNOWLEDGMENTS

We thank Dr. Michael S. Brown for using BOLSIG code to calculate the plasma parameters in the active discharge. We also thank Drs. William Bailey, Alan Garscadden, Sergey Macheret, and Lt. Jack Barnett for their helpful comments and suggestions while reviewing this paper.

[1] I. V. Basargin and G. I. Mishin, Sov. Tech. Phys. Lett. **11**, 85 (1985).
[2] P. Bletzinger, B. N. Ganguly, D. Van Wie, and A. Garscadden, J. Phys. D **38**, R33 (2005).
[3] Y. Z. Ionokh, N. V. Chernysheva, A. P. Yalin, S. O. Marcheret, L. Martinelli, and R. B. Miles (unpublished).
[4] O. W. Greenberg, H. K. Sen, and Y. M. Treve, Phys. Fluids **3**, 379 (1960).
[5] M. Y. Jaffrin, Phys. Fluids **8**, 606 (1965).
[6] P. Bletzinger, B. N. Ganguly, and A. Garscadden, Phys. Rev. E **67**, 047401 (2003).
[7] P. Bletzinger, B. N. Ganguly, and A. Garscadden, IEEE Trans. Plasma Sci. **33**, 342 (2005).
[8] SIGLO Homepage, URL www.siglo-kinema.com/bolsig.htm.
[9] V. Guerra, F. M. Dias, J. Loureiro, P. A. Sá, P. Supiot, C. Dupret, and T. Popov, IEEE Trans. Plasma Sci. **31**, 542 (2003).
[10] J. H. Kiffer and R. W. Lutz, J. Chem. Phys. **44**, 658 (1966).
[11] Y. P. Raizer, *Gas Discharge Physics* (Springer-Verlag, Berlin, 1991), pp. 28 and 200.
[12] A. Lofthus and P. H. Krupenie, J. Phys. Chem. Ref. Data **6**, 113 (1977).
[13] V. Guerra and J. Loureiro, Plasma Sources Sci. Technol. **6**, 361 (1997).
[14] L. G. Piper, J. Chem. Phys. **88**, 231 (1988).
[15] L. G. Piper, J. Chem. Phys. **88**, 6911 (1988).
[16] P. Coakley and N. Hershkowitz, Phys. Fluids **22**, 1171 (1979).
[17] G. S. Chiu and S. A. Cohen, Phys. Rev. Lett. **76**, 1248 (1996).
[18] J. M. Williamson and B. N. Ganguly, Phys. Rev. E **64**, 036403 (2001).
[19] H. S. Maciel and J. E. Allen, J. Plasma Phys. **42**, 321 (1989).
[20] L. Conde, L. F. Ibanez, and C. Ferro-Fontan, Phys. Rev. E **64**, 046402 (2001).
[21] P. Bletzinger, B. N. Ganguly, and A. Garscadden, Phys. Plasmas **7**, 4341 (2000).